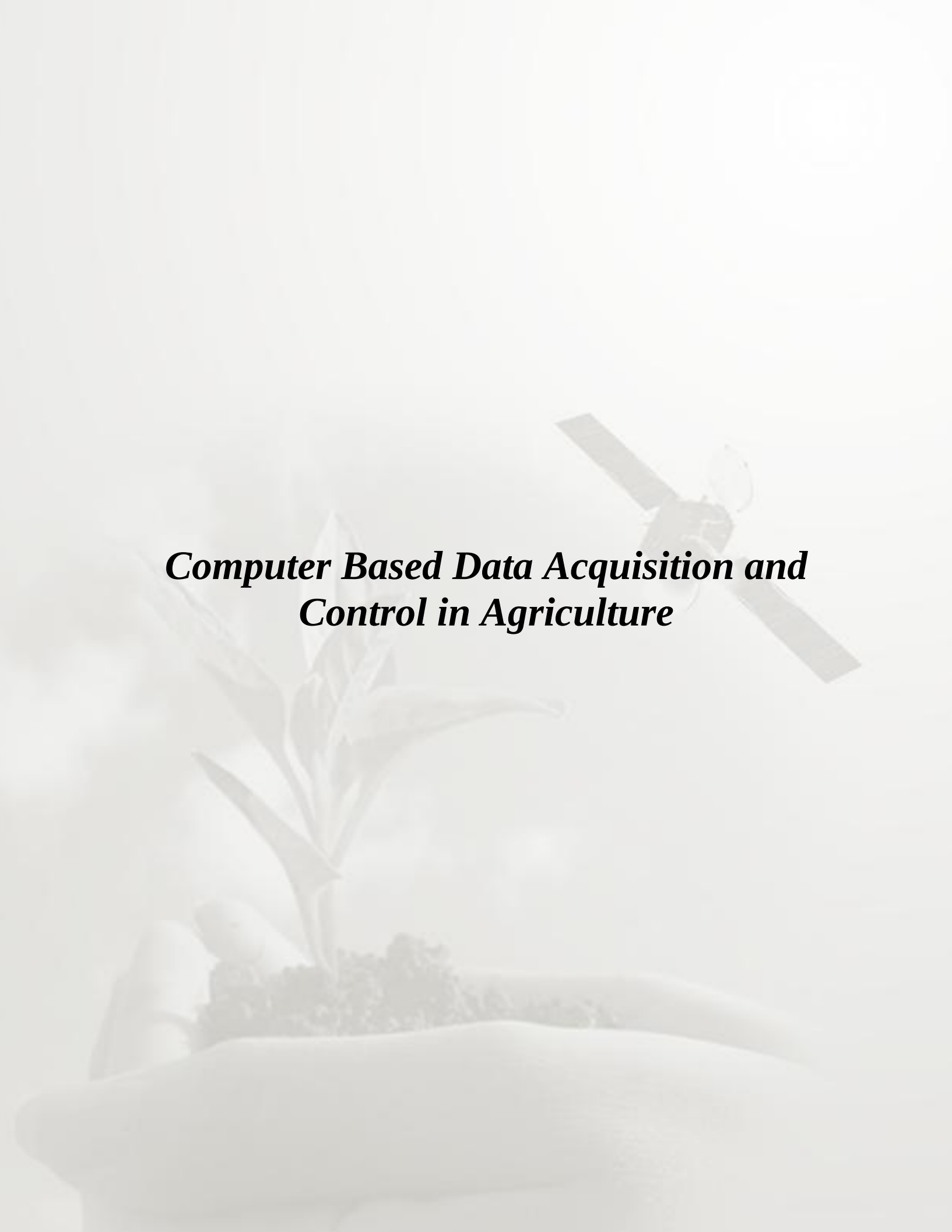

Computer Based Data Acquisition and Control in Agriculture

Development of Nondestructive Detection Algorithm for Internal Defects of Japanese Radish

Kenichi Takizawa[a] , Kazuhiro Nakano[a] , Shintaroh Ohashi[a] , Hiroshi Yoshizawa[a] , Jian Wang[a] , Yasuhumi Sasaki[b]
[a] *Graduate School of Science and Technology*
Niigata University
Niigata, Japan
e-mail: f09m001g@mail.cc.niigata-u.ac.jp

[b] Hiroshi Industry Co., Ltd.
Asahikawa, Japan
e-mail: sasaki@hiroshi.co.jp

***Abstract*—Internal defects always can be found in many produces such as Japanese radish. It is impossible to be detected by human eye. Nondestructive measurement is suitable technique for detecting internal defects like black heart, and air cavity after harvest time, which makes the radish root unmarketable in Japan. This study is aimed to develop the nondestructive detection algorithm for internal defects of radish by near-infrared spectroscopy. Band ratio and linear discriminant analysis were used to build the detection algorithm. In calibration set, the discrimination rate was 94.1% for normal radish, 87.5% for internal defects of radish, and overall success rate was 90.8%. In prediction set, the discrimination rate was 84.4% for normal radish, 95.5% for internal defects of radish, and overall success rate was 89.9%. The first derivative data and neural network system were also used to build the detection algorithm. In training set, the discrimination rate was 100% for normal radish, 82.5% for internal defects of radish, and overall success rate was 94.4%. In testing set, the discrimination rate was 97.8% for normal radish, 77.3% for internal defects of radish, and overall success rate was 91.0%.These results show the potential of the proposed techniques for detecting and predicting radish with internal quality.**

Keywords-component; near-infrared spectroscopy; band ratio; linear discriminant analysis; neural network system; nondestructive detector; Japanese radish; internal defect

I. INTRODUCTION

Production of the Japanese radish comes to 1.6 million tons per year in Japan, the second most harvested vegetable behind the potato. Niigata prefecture is the fourth most planted area of the fall and winter radish. Most of the harvested radishes are shipped to the supplier as raw materials for pickles. This pickle, known as the takuan, is pickled whole without any cutting. Therefore the product value markedly falls when any internal defects are present in the radish. These defects, including black heart and air cavities, make the radish unmarketable.

However, it is impossible to detect these defects with the human eye and therefore a form of nondestructive measurement is desirable to detect internal defects after harvest.

This study describes the development of a nondestructive technique for detection of internal defects in the Japanese radish by visible and near-infrared spectroscopy using linear discriminant analysis or a neural network.

II. MATERIALS AND METHODS

A. Samples

For this study, 228 Japanese radishes (harvested in Akatsuka, Nishi-ku, Niigata-shi) were collected. After the data acquisition, the samples were cut and classified as either "Normal" or "Internal Defects" by visual inspection.

The internal defects differed in both size and color, with two kinds of defect observed: a blackish-brown spot (known as black heart) and air cavities. The black-heart defects, were classified by size (above or below 10mm in diameter). The air cavities were classified by internal color (colorless or black) and were between 1-40mm in diameter (Figure 1).

After classifying the 228 samples by visual inspection, it was found that 130 were normal, 5 had ‘large’ black-heart defects, 25 had ‘small’ black-heart defects, 6 had ‘colorless’ air-cavity defects, and 62 had ‘black’ air-cavity defects. For the following analysis, the 130 normal samples and 62 ‘black’ air-cavity defects were used. Because other classes were few in number, they were not used (TABLE I).

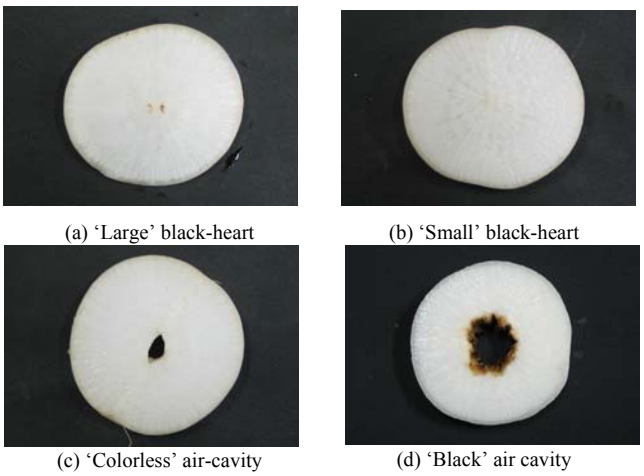

(a) ‘Large’ black-heart (b) ‘Small’ black-heart
(c) ‘Colorless’ air-cavity (d) ‘Black’ air cavity

Figure 1. Cross-section of a sample radish

TABLE I. CLASSIFICATION OF SAMPLES

Class		Number
Normal		130
Internal defects	'Large' black-heart	5
	'Small' black-heart	25
	'Colorless' air-cavity	6
	'Black' air cavity	62

B. *Experimental apparatus*

The experimental apparatus in this study was comprised of a light source, two spectrometers (Handy Lambda II (310-1100 nm) and Solid Lambda NIR 2.2t2 (1000-2150 nm), Spectra Co-op Co., Ltd., Japan), a darkroom and a PC (Figure 2). The optical fiber which connected to the light source was positioned to irradiate one side of the sample radish. On the other side of the sample radish, the optical fiber for light receiving which connected to the spectrometers was positioned to receive transmitted light. The spectrometers were connected with a PC with USB 2.0.

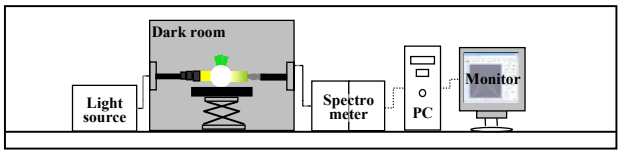

Figure 2. Eperimental apparatus

C. *Spectra data analysis*

The light intensity spectra acquired by the spectrometers were affected by various conditions, such as the sample thickness, light attenuation, and measurement environment. Therefore a reference spectrum (a ceramic plate) and a dark spectrum were obtained and the transmittance calculated by Eq. (1).

$$T = \frac{sample - dark}{reference - dark} \quad (1)$$

where T is the transmittance, and *sample*, *reference*, and *dark* are the light intensities at each wavelength for the sample, reference and dark spectra, respectively.

The absorbance, A, was then calculated by Eq. (2) for the measurement range of 612-825 nm.

$$A = \log_{10}\left(1/T\right) \quad (2)$$

An example of the absorbance spectrum for a normal radish is shown in Figure 3.

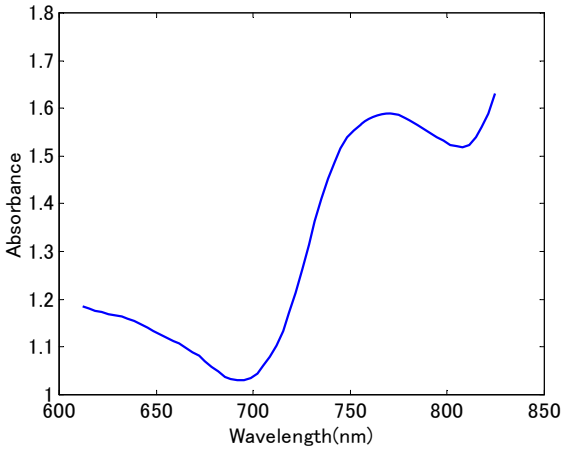

Figure 3. Absorbance spectrum for a normal radish

D. *Dividing into sets for calibration and prediction*

All of the radish data were divided into different sets for calibration and prediction (TABLE II). The calibration set was used for calculation of the linear discriminant and training of the neural network.

TABLE II. THE SETS FOR CALIBRATION AND PREDICTION

	Calibration	Prediction	Overall
Normal	85	45	130
Internal defects	40	22	62
Overall	125	67	192

E. *Linear discriminant analysis*

Linear discriminant analysis was used to discriminate between normal and internal-defect radishes. The band ratio α and β(*BR(α)* and *BR(β)*) were used as the independent variables, and data from the normal and internal-defect radishes were used as the dependent variable. The boundary between the normal and internal-defect sample was defined by the linear discriminant function (3).

$$h_0 + h_1 BR(\alpha) + h_2 BR(\beta) = 0 \quad (3)$$

where h_0 is a constant and h_1 and h_2 are the coefficients of the linear discriminants. The band ratios *BR(α)* and *BR(β)* are given by Eq. (4).

$$BR(\alpha) = A_{a(nm)} / A_{b(nm)}$$
$$BR(\beta) = A_{c(nm)} / A_{d(nm)} \quad (4)$$

where A_a and A_b are the absorbances at a and b in nm. A_c and A_d are the absorbances at c and d in nm. The band ratios for α and β were chosen based on the highest discrimination rate for the normal and internal-defect samples calculated from the absorbance at each measured wavelength.

F. *Nueral network*

The neural network used in this study consists of three layers. The input layer has 59 units, the hidden layer has 50 units, the output layer 2 units (Figure 4).

Input data was obtained as the first derivative of the absorbance at each measured wavelength. For the output, if the data was for a normal radish, then the output neuron was set to 1, and if the data was for an internal-defect radish, then the output neuron was set to 0. Next, the neural network was taken through learning cycles. The learning method was based on error back-propagation learning, using a sigmoid function to represent the characteristics of each neuron. The cognitive error was calculated every cycle and the learning was continued until the cognitive error reached 0.05.

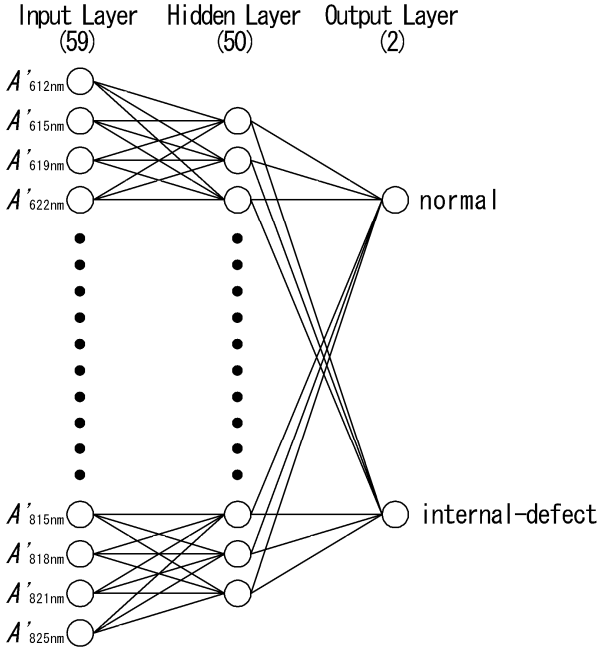

Figure 4. Structure of neural network

III. RESULTS AND DISCUSSION

A. *Linear discriminant analysis*

The linear discriminant function (5) was calculated using the calibration set, which was plotted on a scatter plot of the band ratios for α (horizontal axis) and β (vertical axis). Figure 5 shows the scatter plot along with the linear discriminant function. O indicates data for normal radishes and X data for internal-defect radishes. If the data was plotted above the linear discriminant function, it was defined as normal, and if the data was plotted below the function, it was defined as an internal-defect sample.

Thus, for the calibration set, 80 of the 85 normal radishes were correctly discriminated, giving a discrimination rate of 94.1%. The internal-defect radishes were correctly discriminated for 35 of 40 samples, giving a discrimination rate of 87.5%. As a result, the overall discrimination rate was 92.0% (TABLE III).

The prediction set were also plotted as a scatter plot along with the linear discriminant function (Figure 6). In this set, normal radishes were correctly discriminated for 38 out of 45 samples, giving a discrimination rate of 84.4%, and the internal-defect radishes set were discriminated for 21 out of 22 samples, giving a discrimination rate of 95.5%. As a result, the overall discrimination rate was 88.1% (TABLE III).

$$1.2091 + 0.0308 \times BR(\alpha) + BR(\beta) = 0 \qquad (5)$$

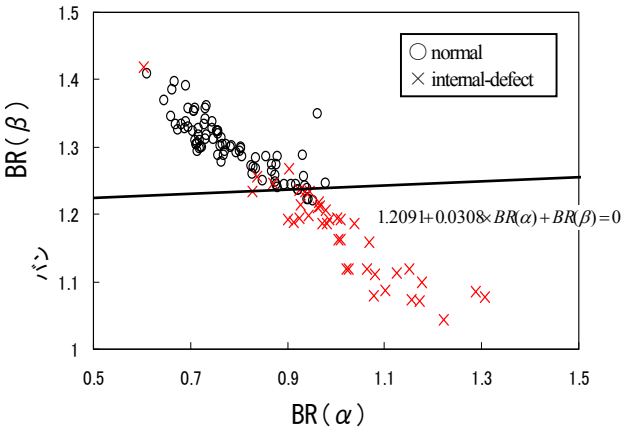

Figure 5. Scatter plot of the band ratios α and β for the calibration set

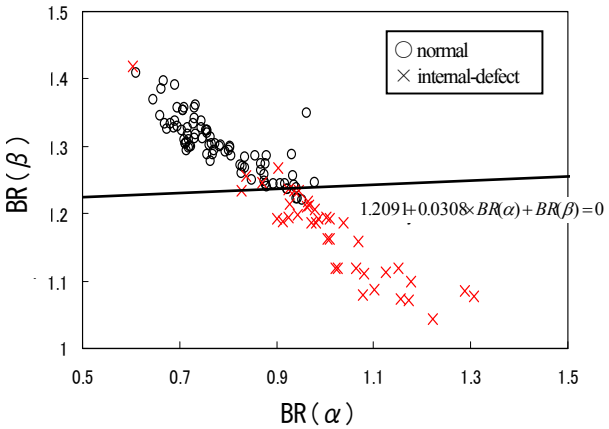

Figure 6. Scatter plot of the band ratios α and β for the prediction set

TABLE III. RESULTS OF LINEAR DISCRIMINANT ANALYSIS

		discrimination rate
Calibration	Normal	94.1% (80/85)
	Internal Defects	87.5% (35/40)
	Total	92.0% (115/125)
Prediction	Normal	84.4% (38/45)
	Internal Defects	95.5% (21/22)
	Total	88.1% (59/67)

TABLE IV. RESULTS OF CLASSIFICATION BY THE NEURAL NETWORK

		discrimination rate
Calibration	Normal	100% (85/85)
	Internal Defects	82.5% (33/40)
	Total	94.4% (118/125)
Prediction	Normal	97.8% (44/45)
	Internal Defects	77.3% (17/22)
	Total	91.0% (61/67)

B. *Nueral network*

For the neural network technique, the learning was continued 89 cycles, at the end of which the cognitive error was 0.0498 (Figure 7).

When the calibration set was entered to this network, the normal radishes were discriminated for 85 out of 85 samples (100% discrimination rate). The internal-defect radishes were discriminated 33 out of 40 samples (82.5%). As a result, the overall discrimination rate was 94.4% (TABLE IV).

When the data for the prediction set was entered into this network, the normal radishes were discriminated 44 out of 45 samples (97.8%). The internal-defect radishes were discriminated for 17 out of 22 samples (77.3%). As a result, overall discrimination rate was 91.0% (TABLE IV).

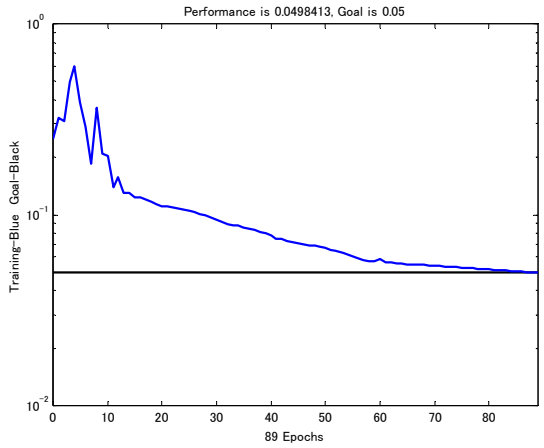

Figure 7. The cognitive error curve in neural network training

IV. CONCLUSION

The linear discriminant analysis shows potential as a technique for detecting and predicting radishes with internal defects using visual and near infrared spectroscopy. Although the discrimination rate for detecting normal radishes was slightly low for the prediction set, we are convinced that enhanced performance can be obtained by tuning the linear discriminant function. Discrimination of radishes using a neural network also shows potential. For both techniques, it is important to obtain as high a discrimination rate as possible for normal radishes, because if the radish is falsely determined to have internal defects it will be wasted. In particular, the results for detection of normal radishes from the prediction set indicated that the techniques are sufficient for practical use.

REFERENCES

[1] K. Nakano, "Application of neural networks to the color grading of apples," Conputers and Electronics in Agriculture, 18(1997), pp.105-116

[2] S. Saranwong, J. Sornsrivichai, S. Kawano, "Prediction of ripe-stage eating quality of mango fruit from its harvest quality measured nondestructively by near infrared spectroscopy," Postharvest Biology and Technology, 31(2004), pp.137-145.

[3] J. Wang, K. Nakano, S. Ohashi, K. Takizawa, J.G. He, "Comparison of differne modes of visible and near-infrared spectroscopy for detecting internal insect infestation in jujubes," Journal of Food Engineering, 101(2010), pp. 78-84.

[4] S. Teerachaichayut, K.Y. Kil, A, Terdwongworakul, W. Thanapase, Y. Nakanishi , "Non-destructive of translucent flesh disorder in intact mangosteen by short wavelength near infrared spectroscopy," Postharvest Biology and Technology, 43(2007), pp. 202-206.

[5] P.N. Schaare, D.G. Fraser, "Comparison of refleatance, interactance and transmission modes of visible-near infrared spectroscopy for measuring internal properties of kiwifruit (Actinidia chinensis)," Postharvest Biology and Technology, 20(2000), pp. 175-184.

[6] V.A. McGlone, P.J. Martinsen, C.J. Clark, R.B. Jordan, "On-line detection of Brownheart in Braeburn apples using near infrared transmission measurements," Postharvest Biology and Technology, 37(2005), pp.142-151.G. Eason, B. Noble, and I. N. Sneddon, "On certain integrals of Lipschitz-Hankel type involving products of Bessel functions," Phil. Trans. Roy. Soc. London, vol. A247, pp. 529–551, April 1955. *(references)*